Phase-Noise Compensation for Spatial-Division Multiplexed Transmission

Arni F. Alfredsson[1], Erik Agrell[1], Henk Wymeersch[1], Magnus Karlsson[2]

[1] *Department of Signals and Systems,* [2] *Department of Microtechnology and Nanoscience,*
Chalmers University of Technology, Gothenburg, SE-412 96, Sweden.
arnia@chalmers.se

Abstract: The problem of correlated phase noise in spatial-division multiplexed transmission is studied. To compensate for the phase noise, an algorithm for joint-core phase-noise estimation and symbol detection is proposed, which outperforms conventional methods.

OCIS codes: (060.2330) Fiber optics communications, (060.1660) Coherent communications

1. Introduction

A promising technology to cope with the ever-increasing demands for data rate in a cost-scalable fashion is spatial-division multiplexing (SDM). This can entail the utilization of, e.g., bundles of single-core fibers (SCFs), multicore fibers (MCFs), or multimode fibers. Moreover, a key concept is the integration of system components, such as optical hardware and digital signal processing. In order to further increase the throughput of these systems, the utilization of advanced modulation formats, such as M-ary quadrature amplitude modulation (M-QAM), is desirable. However, as the order of the modulation grows higher, its sensitivity to phase noise increases.

In the case that local oscillators (LOs) can be shared for all cores in transmission using an MCF or bundles of SCFs, the laser phase noise will be common to the spatial channels. However, due to environmental effects and system imperfections, this common phase noise may decorrelate between the cores over time [1, 2]. This motivates the investigation of joint-core processing for phase-noise compensation. An example is self-homodyne coherent detection (SHCD) [3], or a master–slave configuration in which a single channel is used to estimate the phase noise and the resulting estimates are used for all channels [2]. This may save considerable DSP complexity, but does not improve the phase-noise tolerance compared to processing each channel separately. Conversely, if data on all channels are used jointly to compensate for the phase noise, a substantial improvement can be expected in its tolerance. However, the associated DSP complexity in this case will likely not be as dramatically reduced as in SHCD or the master–slave configuration. At any rate, the problem of joint DSP for phase-noise compensation, with an emphasis on minimizing the bit error rate (BER), has not been addressed in the literature.

In this article, with a focus on minimizing the BER for transmission using an MCF or a bundle of SCFs in the presence of correlated phase noise, we propose an algorithm that performs joint-core processing for phase-noise compensation and symbol detection. The performance of the algorithm is compared to a conventional approach, where each channel is treated separately, for polarization-multiplexed quadrature phase-shift keying (PM-QPSK), PM-16-QAM, and PM-64-QAM multicore transmission, which includes amplified spontaneous emission (ASE) noise and correlated phase noise.

2. System Model

Single-carrier PM transmission of uncoded complex symbols in N_c cores is considered, affected by additive white Gaussian noise (AWGN) and phase noise. The transceiver LOs are assumed to be shared between all cores in an MCF or a bundle of SCFs, giving rise to a common phase noise in all the spatial channels. Moreover, due to possible environmental effects and rotations of the state of polarization, the presence of core- and polarization-dependent phase drifts is assumed, which decorrelates the common laser phase noise between the channels. These drifts are assumed to drift orders of magnitude slower than the laser phase noise [2, 4]. Other linear and nonlinear effects are assumed to have been perfectly compensated for. Further assuming perfect symbol synchronization and one sample per symbol, the discrete-time complex baseband model is written as

$$r_{i,w,k} = s_{i,w,k} e^{j\gamma_{i,w,k}} + n_{i,w,k}, \tag{1}$$

for time index $k = 0, \ldots, N-1$, core index $i = 1, \ldots, N_\mathrm{c}$, and polarization index $w \in \{\mathsf{x}, \mathsf{y}\}$. The number of transmitted symbols per spatial channel is denoted with N, whereas N_c is the number of cores, and x and y are polarization components. The vectors $\boldsymbol{r}_k = [r_{1,\mathsf{x},k}, r_{1,\mathsf{y},k}, \ldots, r_{N_\mathrm{c},\mathsf{x},k}, r_{N_\mathrm{c},\mathsf{y},k}]^T$ contain the received samples in all the channels at times $k = 0, \ldots, N-1$, and form the matrix $\mathbf{R} = [\boldsymbol{r}_0, \boldsymbol{r}_1, \ldots, \boldsymbol{r}_{N-1}] \in \mathbb{C}^{2N_\mathrm{c} \times N}$. Similarly, the matrix $\mathbf{S} =$

$[\boldsymbol{s}_0, \boldsymbol{s}_1, \ldots, \boldsymbol{s}_{N-1}] \in \mathbb{C}^{2N_\mathrm{c} \times N}$ contains all the transmitted symbols, where $\boldsymbol{s}_k = [s_{1,\mathrm{x},k}, s_{1,\mathrm{y},k}, \ldots, s_{N_\mathrm{c},\mathrm{x},k}, s_{N_\mathrm{c},\mathrm{y},k}]^T$. Finally, the noise matrix $\mathbf{N} = [\boldsymbol{n}_0, \boldsymbol{n}_1, \ldots, \boldsymbol{n}_{N-1}] \in \mathbb{C}^{2N_\mathrm{c} \times N}$, where $\boldsymbol{n}_k = [n_{1,\mathrm{x},k}, n_{1,\mathrm{y},k}, \ldots, n_{N_\mathrm{c},\mathrm{x},k}, n_{N_\mathrm{c},\mathrm{y},k}]^T$, contains independent and identically distributed, circularly symmetric complex Gaussian components, and models the ASE in all the channels. The transmitted symbols are drawn uniformly from a complex constellation $\mathcal{X} \in \mathbb{C}$, which is subject to an energy constraint such that the average symbol energy is E_s. Pilot symbols are distributed with regular intervals between the data symbols on each channel, with the x-polarization in core 1 having a greater pilot overhead than the rest of the channels.

The total phase noise per spatial channel consists of a sum of the laser phase noise, a core-dependent phase drift, and a polarization-dependent phase drift, which are all modelled as Gaussian random-walks with innovation variances σ_θ^2, σ_δ^2, and σ_ε^2, respectively. Specifically, the laser phase noise innovation variance is defined as $\sigma_\theta^2 = 2\pi\Delta\nu T_\mathrm{s}$, where $\Delta\nu$ is the total laser linewidth and T_s is the symbol duration. The total phase noise in all the channels at time k is encapsulated in $\boldsymbol{\gamma}_k = [\gamma_{1,\mathrm{x},k}, \gamma_{1,\mathrm{y},k}, \ldots, \gamma_{N_\mathrm{c},\mathrm{x},k}, \gamma_{N_\mathrm{c},\mathrm{y},k}]^T$. Further, $\boldsymbol{\Gamma} = [\boldsymbol{\gamma}_0, \boldsymbol{\gamma}_1, \ldots, \boldsymbol{\gamma}_{N-1}] \in \mathbb{R}^{2N_\mathrm{c} \times N}$ describes a $2N_\mathrm{c}$-dimensional Gaussian random walk, i.e., $\boldsymbol{\gamma}_k = \boldsymbol{\gamma}_{k-1} + \boldsymbol{\Delta}_k$, with $\boldsymbol{\gamma}_0$ uniformly distributed on $[0, 2\pi)^{2N_\mathrm{c}}$. The innovation is a correlated Gaussian random vector, $\boldsymbol{\Delta}_k \sim \mathcal{N}(\mathbf{0}, \mathbf{Q})$, where $\mathbf{Q} \in \mathbb{R}^{2N_\mathrm{c} \times 2N_\mathrm{c}}$ is a known matrix and is defined as

$$\mathbf{Q} = \begin{bmatrix} \mathbf{Q}_1 & \mathbf{Q}_2 & \mathbf{Q}_2 & \cdots & \mathbf{Q}_2 \\ \mathbf{Q}_2 & \mathbf{Q}_1 & & & \vdots \\ \mathbf{Q}_2 & & \ddots & & \vdots \\ \vdots & & & \ddots & \mathbf{Q}_2 \\ \mathbf{Q}_2 & \cdots & \cdots & \mathbf{Q}_2 & \mathbf{Q}_1 \end{bmatrix}, \quad \mathbf{Q}_1 = \begin{bmatrix} \sigma_\theta^2 + \sigma_\delta^2 + \sigma_\varepsilon^2 & \sigma_\theta^2 + \sigma_\delta^2 \\ \sigma_\theta^2 + \sigma_\delta^2 & \sigma_\theta^2 + \sigma_\delta^2 + \sigma_\varepsilon^2 \end{bmatrix}, \quad \mathbf{Q}_2 = \begin{bmatrix} \sigma_\theta^2 & \sigma_\theta^2 \\ \sigma_\theta^2 & \sigma_\theta^2 \end{bmatrix}. \tag{2}$$

The phase noise is statistically independent of the transmitted symbols and the AWGN. Furthermore, it is unknown to both the transmitter and the receiver.

3. Proposed Algorithm

By using the factor graph framework and the sum–product algorithm [5], the detector that minimizes the BER, namely, the maximum *a posteriori* detector, can be realized for the channel model in (1). However, the direct implementation of the resulting equations is impractical since it requires many integrals to be carried out. Thus, approximations are needed, and multiple solutions have been proposed in the literature. A particular approximation results in an excellent performance–complexity tradeoff, namely to constrain the *a posteriori* phase-noise PDFs to be in a family of Tikhonov distributions. This approach was originally proposed in [6], and recently extended for a polarization-multiplexed transmission in a single-core fiber [7]. In this work we extend the method further to account for multicore fibers with core- and polarization-dependent phase drifts and shared laser phase noise between the cores. The main difference from [7] lies in the presence of these additional drifts that decorrelate the common laser phase noise between the spatial channels, and hence impose difficulties in its estimation. Hereafter, this algorithm will be referred to as Tikhonov Joint Estimator–Detector (TJED). For more details on the algorithm derivation for single-channel or polarization-multiplexed transmission, the reader is referred to [6, 7].

4. Performance Analysis

The performance of the proposed algorithms is assessed through Monte Carlo simulations of PM-QPSK, PM-16-QAM, and PM-64-QAM multicore transmission in the presence of correlated phase noise. Bits are Gray encoded prior to bit-to-symbol mapping, and no forward error correction is used. 7- and 19-core transmission are assumed, resulting in parallel transmission of 14 and 38 spatial channels, respectively. The number of transmitted symbols in each channel is at most $N = 200\,000$. For each result, blocks of symbols are repeatedly transmitted and bit errors are accumulated until the total number of errors exceeds 1000. The average pilot overhead over all the channels is 5%, and every pilot is normalized such that its energy is E_s. The proposed algorithm, running 2 iterations, is compared to a conventional phase-noise compensation scheme, namely, running the blind phase search (BPS) algorithm [8] separately on each channel with differential encoding applied.

The comparison pertains to the phase-noise tolerance of the algorithms. To that end, the BER is computed as a function of different amounts of laser linewidth and symbol duration products, $\Delta\nu T_\mathrm{s}$. The signal-to-noise (SNR) per information bit is fixed such that a BER of 10^{-3} is obtained for pilot-free transmission in the absence of phase noise. Hence, BER penalty due to imperfect phase-noise compensation as well as pilot overhead will occur. In addition to evaluating the algorithms for a range of $\Delta\nu T_\mathrm{s}$, results are obtained for two different amounts of phase-noise decor-

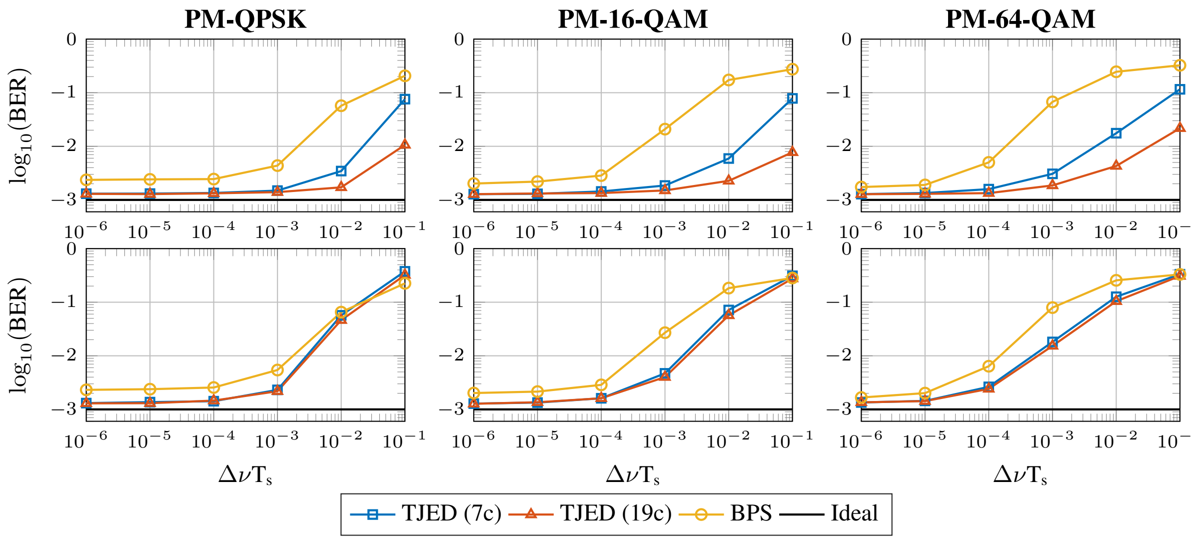

Fig. 1: Phase-noise tolerance of TJED for 7- and 19-core transmission at a fixed SNR per information bit and pilot overhead, with the core- and polarization-dependent phase drifts 1000 times (top 3 plots) and 10 times (bottom 3 plots) slower than the laser phase noise.

relation between the spatial channels. This is controlled by the speed of the core- and polarization-dependent phase drifts, relative to the laser phase noise.

Fig. 1 shows the results for $\sigma_\delta^2 = \sigma_\varepsilon^2 = \sigma_\theta^2/1000$ (top) and $\sigma_\delta^2 = \sigma_\varepsilon^2 = \sigma_\theta^2/10$ (bottom), where all plots include an ideal curve that corresponds to no penalty due to phase noise. The proposed algorithm outperforms the conventional approach in most cases. Furthermore, TJED attains similar or lower BER for all the tested laser linewidths when the number of cores is increased, resulting in a higher linewidth tolerance. In general, the performance improvements are more pronounced when $\sigma_\delta^2 = \sigma_\varepsilon^2 = \sigma_\theta^2/1000$. This is to be expected since slower core- and polarization-dependent drifts result in less decorrelation in the common laser phase noise, which allows for a more effective phase-noise compensation. In particular, for 19-core transmission and $\sigma_\delta^2 = \sigma_\varepsilon^2 = \sigma_\theta^2/1000$, TJED tolerates at least 45 times higher linewidth compared to the conventional method before exceeding BER of 10^{-2}.

Increasing the pilot overhead results in a higher linewidth tolerance but raises the required SNR per information bit, whereas lowering the overhead has the opposite effect. Finally, it is worth noting that the estimated computational complexity per channel of the proposed algorithm depends on the modulation format order and number of cores. More specifically, it is higher than the estimated complexity of the algorithm in [7, Sec. IV-D] by a factor of approximately 3 for the tested modulation formats and number of cores, in terms of the number of real multiplications and additions.

5. Conclusion

A novel algorithm was proposed for joint-core phase-noise compensation, when the system is affected by laser phase noise in addition to core- and polarization-dependent phase drifts. The performance analysis shows that the algorithm outperforms a conventional approach, having tolerance for at least 45 times higher laser linewidth in certain scenarios. This makes it an appealing option for spatial-division multiplexed fiber-optical communication systems, employing LOs that are shared between cores.

References

1. R. S. Luís *et al.*, "Comparing inter-core skew fluctuations in multi-core and single-core fibers," in "Proc. Lasers and Electro-Optics," (2015), pp. 1–2.
2. M. D. Feuer, L. E. Nelson, X. Zhou, S. L. Woodward, R. Isaac, B. Zhu, T. F. Taunay, M. Fishteyn, J. M. Fini, and M. F. Yan, "Joint digital signal processing receivers for spatial superchannels," IEEE Photonics Technol. Lett. **24**, 1957–1960 (2012).
3. B. J. Puttnam *et al.*, "Investigating self-homodyne coherent detection in a 19 channel space-division-multiplexed transmission link," Opt. Express **21**, 1561–1566 (2013).
4. M. Karlsson, "Four-dimensional rotations in coherent optical communications," J. Lightw. Technol. **32**, 1246–1257 (2014).
5. F. R. Kschischang, B. J. Frey, and H.-A. Loeliger, "Factor graphs and the sum-product algorithm," IEEE Trans. Inf. Theory **47**, 498–519 (2001).
6. G. Colavolpe, A. Barbieri, and G. Caire, "Algorithms for iterative decoding in the presence of strong phase noise," IEEE J. Sel. Areas Commun. **23**, 1748–1757 (2005).
7. A. F. Alfredsson, R. Krishnan, and E. Agrell, "Joint-polarization phase-noise estimation and symbol detection for optical coherent receivers," J. Lightw. Technol. **34**, 4394–4405 (2016).
8. T. Pfau, S. Hoffmann, and R. Noé, "Hardware-efficient coherent digital receiver concept with feedforward carrier recovery for M-QAM constellations," J. Lightw. Technol. **27**, 989–999 (2009).